

Critical Resistance of the Quantum Hall Ferromagnet in AlAs 2D Electrons

E. P. De Poortere, E. Tutuc, and M. Shayegan

Department of Electrical Engineering, Princeton University, Princeton, New Jersey 08544

(Dated: May 22, 2019)

Magnetic transitions in AlAs two-dimensional electrons give rise to sharp resistance spikes within the quantum Hall effect. Such spikes are likely caused by carrier scattering at magnetic domain walls below the Curie temperature. We report a critical behavior in the temperature dependence of the spike width and amplitude, from which we deduce the Curie temperature of the quantum Hall ferromagnet. Our data also reveal that the Curie temperature increases monotonically with carrier density.

Various forms of order have been shown to derive from or compete with the quantum Hall (QH) state in two-dimensional (2D) electron systems, including charge density waves, the Wigner crystal, stripe and bubble phases, and liquid crystal states. Recent experimental evidence, often in the form of magnetic hysteresis, also points to the existence of a ferromagnetic phase within the integer and fractional QH states [1, 2, 3, 4, 5, 6, 7, 8, 9, 10, 11]. The analogy with spontaneous polarization in conventional Ising ferromagnets exists when two Landau levels (LL's) with opposite spin quantum numbers and different orbital indices are degenerate. Experimentally, this LL coincidence is obtained by tilting the normal of the sample at an angle θ with respect to the magnetic field. Exchange energy ensures that at temperature $T = 0$, one of the two crossing levels is fully occupied and the other empty. Therefore, as a function of increasing magnetic field, the 2D system undergoes a first-order transition caused by the crossing LL's [Fig. 1(c), inset], and magnetic domains form at the transition. The electronic state within each domain is thus described as an Ising-like QH ferromagnet with either one of two possible spin orientations. In materials such as AlAs [7], (Cd,Mn)Te [10], InGaAs [1], InSb [11], and wide GaAs quantum wells [9], LL crossings and the associated magnetic domains lead to resistance maxima within the integer QH or Shubnikov-de Haas minima of the magnetoresistance (R_{xx}) [Fig. 1(a)], while in GaAs 2D electrons, sharp resistance peaks are observed in the fractional QH R_{xx} minima. In the latter case, the spikes are caused by crossing LL's of composite fermions [8].

Theorists have begun to address the nature of domain boundaries in Ising QH ferromagnets [12, 13, 14], though no calculation of the domain wall resistance in these systems exists at present. Estimates for the domain wall energies, however, yield the Curie temperature of the ferromagnet [12], which can be determined experimentally. Determination of this temperature is the first objective of our work. Furthermore, AlAs resistance spikes can be separated fairly easily from the background resistance of the 2D system, so that they provide a direct measure of the domain wall magnetoresistance. Measurements of the resistance spike dimensions, namely its amplitude (ΔR_{sp}) and width in magnetic field (ΔB_{sp}) [see

Fig. 1(b)], therefore supply an experimental basis against which future models of the domain walls can be tested, and provide a second motivation for our study.

In this Letter, we report temperature- and density-dependence measurements of the resistance spikes in AlAs 2D electrons. Our results reveal that: (1) ΔR_{sp} increases with T up to a characteristic temperature, T_M , beyond which it decreases with T ; (2) below the same temperature T_M , ΔB_{sp} is relatively constant, while above T_M , ΔB_{sp} increases significantly with temperature; (3) T_M increases with the 2D electron density (n). Comparing the temperature dependence of the spike width with that expected from a mean-field 2D Ising model, we are able to identify T_M with the Curie temperature of the QH ferromagnet.

AlAs offers several advantages for the study of QH ferromagnets: first, the band g -factor of 2D electrons in AlAs is approximately 2 [15], while the effective electron masses (at the X points of the Brillouin zone) are 1.1 and 0.19 in the longitudinal and transverse directions, respectively [16]. The latter properties ensure that the Zeeman (E_Z) and cyclotron (E_c) energies are comparable in magnitude for low values of θ , a regime in which the orbital effect of the tilted field can be neglected [12]. Second, the high quality of our AlAs quantum wells (QW's), in which we have observed developing fractional QH states at high-order fillings [17], implies that the interparticle Coulomb interaction, rather than disorder, dominates the ground state of the 2D system.

The sample studied here is a 150 Å-wide AlAs QW surrounded by $\text{Al}_{0.4}\text{Ga}_{0.6}\text{As}$ barriers, modulation-doped on the front side with Si, and grown by molecular beam epitaxy on a GaAs (100) substrate. For magnetotransport measurements, a $100 \times 325\mu\text{m}$ Hall bar was lithographically etched on the sample surface, and 1500 Å-thick Au-GeNi contacts were deposited and alloyed at 440 °C for 10 minutes in forming gas. Front and back gates were fitted to the sample. Experiments were performed in pumped ^3He and dilution refrigerators in magnetic fields up to 18 T. Prior to measurements, the sample was illuminated with a red LED at $T \simeq 4$ K, while a positive bias was applied between the back gate and the 2D system. This procedure is required to make Ohmic contact to the 2D system in our sample, and is detailed in [18].

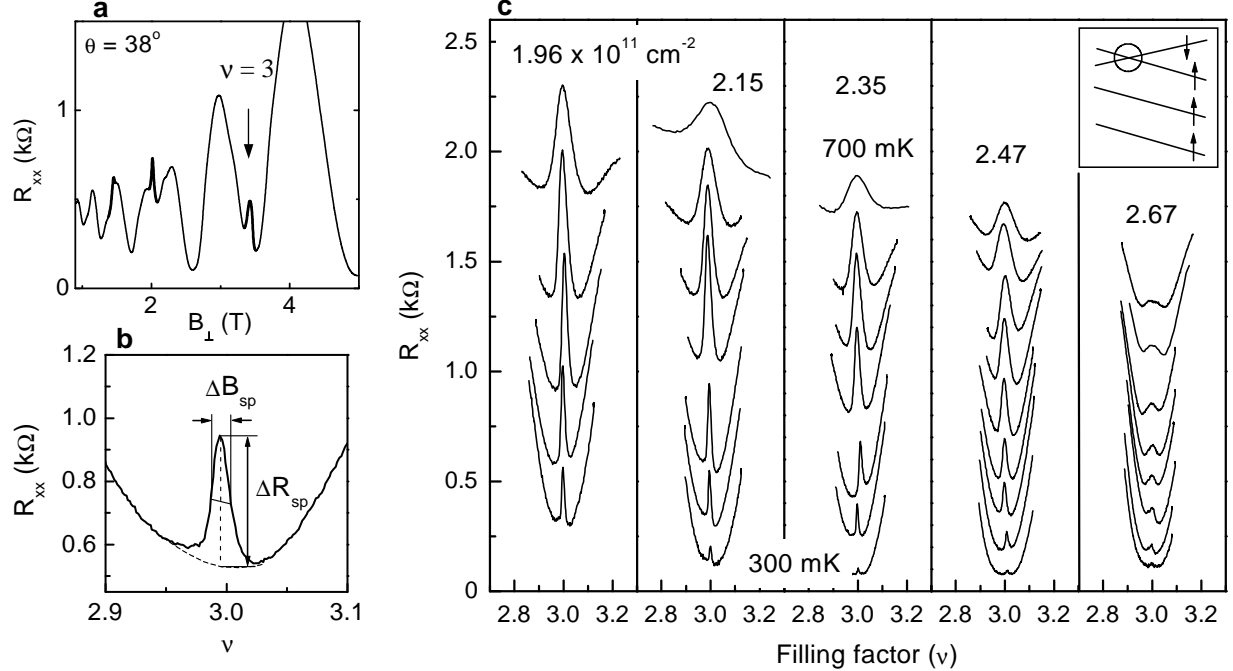


FIG. 1: (a) Magnetoresistance of AlAs 2D electrons for $n = 2.5 \times 10^{11} \text{ cm}^{-2}$, showing resistance spikes at LL crossings near $\nu = 3$ and 5. (b) Definition of the spike amplitude (ΔR_{sp}) and linewidth (ΔB_{sp}). (c) Magnetoresistance of AlAs 2D electrons near $\nu = 3$, showing the resistance spike for different carrier densities (n) and temperatures ($300 \lesssim T \lesssim 700 \text{ mK}$). From left to right, tilt angles are $\theta = 16^\circ, 25^\circ, 30^\circ, 34^\circ$, and 37° . Note the strong suppression of the spike amplitude as n increases. For clarity, only data for downward B sweeps are shown. Inset schematically shows the crossing of opposite spin Landau levels at $\nu = 3$.

Figure 1(a) gives an overview of the sample magnetoresistance for $n = 2.5 \times 10^{11} \text{ cm}^{-2}$ and $\theta = 38^\circ$, showing the resistance spikes near $\nu = 3$ and 5. The T and n dependence of the $\nu = 3$ spike are given in Fig. 1(c) [19]. From these data we first plot, in Fig. 2, the spike amplitudes as a function of T . We see that ΔR_{sp} reaches a maximum at a temperature T_M , and that T_M increases monotonically with n (inset of Fig. 2). Furthermore, ΔR_{sp} decreases quickly as the density increases; for $n \gtrsim 2.7 \times 10^{11} \text{ cm}^{-2}$ in this sample, the spike amplitude is too small to be measured. On the other hand, at the lowest measured density, the maximum ΔR_{sp} is about 700Ω , comparable to the R_{xx} maxima at half-integer ν , when the Fermi level lies close to the energies of extended states. We note that an even stronger resistance spike is seen near $\nu = 4$ in this sample: its ΔR_{sp} is more than twice the magnitude of the neighboring R_{xx} maxima at or near half-integral fillings. The large magnitude of ΔR_{sp} at low n and near $\nu = 4$ indicates that the scattering process at the resistance spike is fundamentally different from that present in the sample when the Fermi level nearly coincides with that of an extended state.

The T dependence of the spike width, ΔB_{sp} , is plotted for two different densities in Figs. 3(a) and (b). Both graphs show that ΔB_{sp} decreases as the 2D electrons cool down, and tends to saturate below a given temperature

that depends on the density. Although ΔB_{sp} depends smoothly on T , the onset of its rise with T appears to occur near T_M , the temperature at which ΔR_{sp} is maximum. More quantitatively, a threshold temperature can be defined for the $\Delta B_{sp}(T)$ data in Figs. 3(a) and (b), by first fitting straight lines to the low- and high- T ranges, and taking the intersection of these lines. In Fig. 3(a), the resulting T is 500 mK, a value very close to T_M . This correspondence suggests a common physical process for the T dependencies of both ΔR_{sp} and ΔB_{sp} .

In order to better understand our data, we use a Bragg-Williams model [21] applied to a system composed of two energy levels with respective relative fillings f_1 and f_2 , corresponding to the highest occupied level and the lowest unoccupied level at $\nu = 3$. We define the magnetization (m_z) as $m_z = f_1 - f_2$, so that $m_z = 1$ (-1) if the first (second) level is fully occupied. The electron energy can then be written as $E(m_z) = bm_z - \frac{1}{2}Jm_z^2$, where b is a reduced magnetic field that includes contributions from single-particle energies (E_Z and E_c) and from interactions, and J is an effective interaction strength [22]. The free energy of the 2D system is given by

$$F(b, m_z) = -TS(m_z) + E(b, m_z), \quad (1)$$

where $S(m_z)$ is the mixing entropy of the two phases. For every b and T , we minimize F with respect to m_z , and

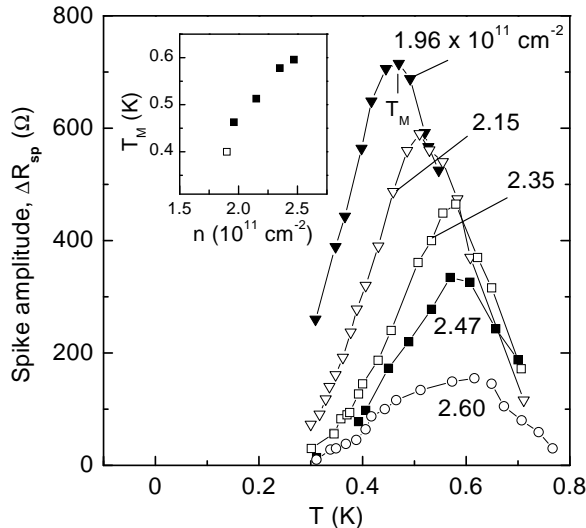


FIG. 2: Plots of the resistance spike amplitude (ΔR_{sp}) vs. T , for several carrier densities. Inset: Temperatures of the ΔR_{sp} maxima as a function of n . (full squares: from this Figure; hollow square: data from a separate cooldown.)

thus obtain the equilibrium magnetization. The model predicts that for $T < T_C = J$ (the Curie temperature), two different m_z 's minimize F , and that the system divides into magnetic domains.

Above the Curie point, the transition in field becomes increasingly gradual as T increases, as we see by calculating the field (b_+) at which the equilibrium m_z equals a given threshold value, say $-1/2$. We obtain:

$$b_+(T) = -0.5T_C + 0.55T \quad (T > T_C). \quad (2)$$

This b_+ corresponds to an intermediate state between the transition ($m_z = 0$) and full polarization ($m_z = -1$), so that we expect b_+ to be related to the spike width. Plotting $\Delta b = 2b_+(T)$ in the inset of Fig. 3(b), we see that this parameter vanishes at T close to T_C (i.e., at $T = 0.91T_C$), and increases for larger T . This behavior is similar to that of the measured ΔB_{sp} , suggesting that the threshold temperatures in Figs. 3(a) and (b) are the Curie temperatures of the QH ferromagnet at the respective carrier densities. An implication of our analysis is that $T_M \simeq T_C$, since the peak in $\Delta R_{sp}(T)$ agrees with the temperature threshold of $\Delta B_{sp}(T)$.

The fact that the ΔR_{sp} maximum occurs near T_C is qualitatively consistent with calculations of the critical resistance in ferromagnetic semiconductors [23, 24]. According to these calculations, the diverging correlation length of spin fluctuations as $T \rightarrow T_C$ causes a peak resistance at a temperature T_M close to T_C , with $|T_M - T_C|/T_C \sim 10^{-5}$ in typical semiconductors [24]. Although the origin of scattering at the spike in our system is unclear at present, data in Fig. 2 qualitatively confirm the predicted peak resistance at T_C . We also note that

we obtain similar empirical correspondences between the T dependencies of ΔR_{sp} and ΔB_{sp} for $n = 2.35$ and $2.47 \times 10^{11} \text{ cm}^{-2}$, two other densities for which the data ranges are large enough for comparison to be possible.

In the inset of Fig. 2, we plot the density dependence of T_M deduced from the ΔR_{sp} peaks in Fig. 2. Within the small density range allowed by our experiment, we observe that T_M increases with n . This is consistent with our expectation that T_C ($\simeq T_M$), through the exchange interaction, should scale with the Coulomb energy, $e^2/4\pi\epsilon l_B$, which increases with B_\perp [$\epsilon \simeq 10\epsilon_0$ is the dielectric constant of AlAs and $l_B = (\hbar/eB_\perp)^{1/2}$ is the magnetic length] [25]. The values we obtain for T_C also agree with the estimate (~ 500 mK) calculated by Jungwirth and MacDonald for the Curie temperature of AlAs 2D electrons at $n = 2.5 \times 10^{11} \text{ cm}^{-2}$ [12].

Plotted in Fig. 3(a) are the ΔR_{sp} and ΔB_{sp} data for both upward and downward B sweeps. These values, which depend on the sweep direction at sufficiently low T , reflect the observed R_{xx} hysteresis (which mostly occurs in amplitude rather than in field). Figure 3(a) shows that the temperature corresponding to the onset of hysteresis is *lower* than the Curie temperature derived from the $\Delta R_{sp}(T)$ and $\Delta B_{sp}(T)$ dependencies. This implies that magnetic domains present (below T_C) at the LL crossing do not necessarily give rise to hysteretic R_{xx} . Furthermore, the strength of hysteresis depends on sample cooldown, while T_C as defined above does not show such sensitivity, suggesting that hysteresis is controlled by cooldown-dependent parameters such as the precise nature of impurity disorder.

Although the T and n dependencies described in our work apply to resistance spikes at $\nu = 3$, we have obtained similar data for LL crossings at other filling factors, though in a less complete manner. The T dependencies of ΔR_{sp} and ΔB_{sp} for the spike near $\nu = 5$, e.g., are analogous to our $\nu = 3$ spike data; the amplitude of the spike at $\nu = 4$ (at $T = 30$ and 300 mK) also decreases monotonically as n increases. Spike measurements at $\nu = 4$ and 5 are thus qualitatively consistent with results obtained from the $\nu = 3$ spike.

We now outline the main differences between our work and that of Jaroszyński *et al.* [10], who recently performed a detailed study of resistance spikes in (Cd,Mn)Te quantum wells. First, authors in Ref. [10] determine T_C from the temperature at which the *total* value of the resistance at the spike (R_{tot}) reaches a maximum, whereas we treat the spike *amplitude* ΔR_{sp} as the physical parameter reflecting the contribution of the domains (or, near T_C , of the spin fluctuations) to the total resistance. Second, the onset of hysteresis in Ref. [10] matches the peak in $R_{tot}(T)$ (for one of the measured densities). In our samples, as can be seen in Fig. 1(c), R_{tot} increases monotonically with T , so that the peak in $R_{tot}(T)$, if it exists, occurs at $T > 700$ mK, i.e., at a much higher T than the onset of spike hysteresis [26]. Third, T_C determined in

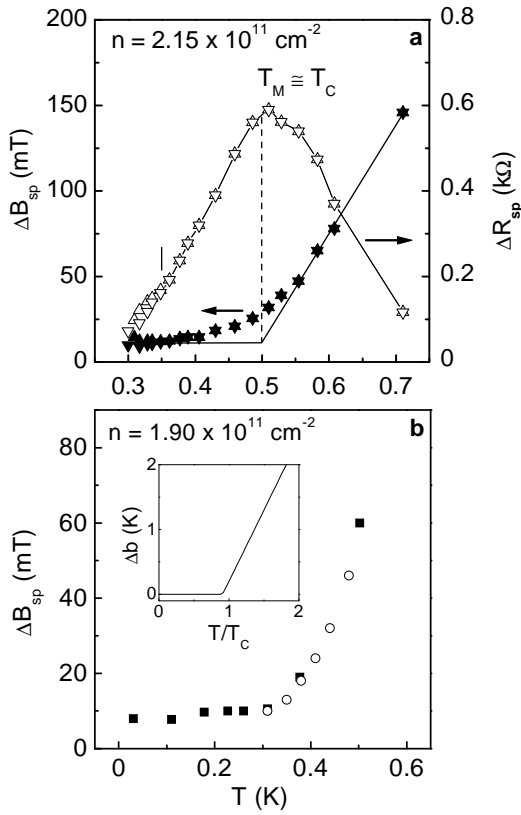


FIG. 3: (a) ΔR_{sp} and ΔB_{sp} vs. T , showing the correspondence between the threshold temperature in $\Delta B_{sp}(T)$ with T_M , the temperature of the ΔR_{sp} maximum. T_M is interpreted as the Curie temperature of the QH ferromagnet (T_C). Upward- and downward-pointing triangles represent data from up and down field sweeps respectively, and show that the onset of hysteresis (vertical mark at $T = 350$ mK) is significantly lower than $T_M \simeq T_C$. (b) $\Delta B_{sp}(T)$ for $n = 1.90 \times 10^{11} \text{ cm}^{-2}$, showing ΔB_{sp} independent of T at low temperatures, and increasing with T for $T \gtrsim 400$ mK. Full and hollow symbols are used to distinguish data from two different cooldowns. Inset: spike width predicted by Bragg-Williams theory, displaying a behavior qualitatively similar to that of the measured $\Delta B_{sp}(T)$. T_C in this graph is the Curie temperature of the Ising ferromagnet.

Ref. [10] decreases with increasing n , a trend that is contrary to our experimental results and unexpected based on theoretical grounds. While we do not understand the origin of these various differences between spikes in AlAs and (Cd,Mn)Te, we emphasize that the latter contains magnetic Mn ions that may play a role in the formation of magnetic domains, while AlAs is nonmagnetic.

In conclusion, we have observed critical behaviors (at matching temperatures) in both the amplitude and the linewidth of the resistance spikes in the AlAs QH ferromagnet, and determined from these the Curie temperature of the ferromagnet. The critical behaviors are qualitatively consistent with the results of two independent models: the observed peak in $\Delta R_{sp}(T)$ is predicted

by calculations of the critical resistance in ferromagnetic semiconductors, and the measured $\Delta B_{sp}(T)$ dependence can be understood by a mean-field analysis of the Ising model.

This work was supported by the Princeton University NSF MRSEC grant. We acknowledge fruitful discussions with Ravin Bhatt, Duncan Haldane, and Allan MacDonald, and thank Eric Palm and Tim Murphy for their technical assistance. Part of this work was performed at the National High Magnetic Field Laboratory in Tallahassee, FL, which is also supported by the NSF.

- [1] S. Koch *et al.*, Phys. Rev. B **47**, 4048 (1993).
- [2] A.J. Daneshvar *et al.*, Phys. Rev. Lett. **79**, 4449 (1997).
- [3] T. Jungwirth *et al.*, Phys. Rev. Lett. **81**, 2328 (1998).
- [4] H. Cho *et al.*, Phys. Rev. Lett. **81**, 2522 (1998).
- [5] V. Piazza *et al.*, Nature **402**, 638 (1999).
- [6] J. Eom *et al.*, Science **289**, 2320 (2000).
- [7] E.P. De Poortere *et al.*, Science **290**, 1546 (2000).
- [8] J. Smet *et al.*, Phys. Rev. Lett. **86**, 2412 (2001).
- [9] K. Muraki *et al.*, Phys. Rev. Lett. **87**, 196801 (2001).
- [10] J. Jaroszyński *et al.*, Phys. Rev. Lett. **89**, 266802 (2002).
- [11] J.-C. Chokomakoua, N. Goel, S.-K. Cheong, M. Santos, S. Murphy, Bull. Am. Phys. Soc. **48**, 462 (2003).
- [12] T. Jungwirth and A.H. MacDonald, Phys. Rev. Lett. **87**, 216801 (2001).
- [13] L. Brey and C. Tejedor, Phys. Rev. B **66**, 041308 (R) (2002).
- [14] J.T. Chalker *et al.*, Phys. Rev. B **66**, 161317 (2002).
- [15] H.W. van Kesteren *et al.*, Phys. Rev. B **39**, 13426 (1989).
- [16] S. Adachi, J. Appl. Phys. **58**, R1 (1985).
- [17] E.P. De Poortere *et al.*, Appl. Phys. Lett. **80**, 1583 (2002).
- [18] E.P. De Poortere *et al.*, Phys. Rev. B (in press).
- [19] For each n and T in Fig. 1(c), the tilt angle was chosen so that the transition (i.e., the resistance spike) would occur as close to $\nu = 3$ as possible. This angle turning is necessary because for a fixed tilt angle, the spike shifts to slightly lower B as T increases. In practice, the angle tuning we perform to keep the spike at $\nu = 3$ results in a 3 % shift of the spike field. To first order, the spike field can be considered constant.
- [20] E.P. De Poortere *et al.*, Physica E **12**, 36 (2002).
- [21] P. M. Chaikin and T. C. Lubensky, *Principles of Condensed Matter Physics* (Cambridge University Press, Cambridge, UK, 1995), p. 144.
- [22] T. Jungwirth and A.H. MacDonald, Phys. Rev. B **63**, 035305 (2001).
- [23] P.G. de Gennes and J. Friedel, J. Phys. Chem. Solids **4**, 71 (1958).
- [24] S. Alexander, J.S. Helman, and I. Balberg, Phys. Rev. B **13**, 304 (1976), and references therein.
- [25] For approximate values of exchange-correlation energies of 2D electrons in a magnetic field, see, for example, A.H. MacDonald and D. S. Ritchie, Phys. Rev. B **33**, 8336 (1986).
- [26] Furthermore, resistance spikes in our samples are mostly hysteretic in *amplitude* (and width) rather than in *field*. (Cd,Mn)Te spikes in Ref. [10] are hysteretic in field only.